Core-excited metastable levels: application to spectroscopy, to the generation of picosecond extreme-ultraviolet pulses, and to lasers

S. E. Harris and J. F. Young

Edward L. Ginzton Laboratory, Stanford University, Stanford, California 94305

The paper reviews both the properties and the applications of core-excited metastable atoms. The production of these atoms by microwaves, pulsed hollow-cathode discharges, and laser-produced x rays is described. We discuss the application of these atoms to several new types of spectroscopy that allow autoionizing linewidths as narrow as 0.1 cm^{-1} to be measured. The application of these metastables to the generation of picosecond-time-scale soft-x-ray pulses and to XUV lasers is also discussed.

1. INTRODUCTION

Metastable levels of atoms and ions have played an important and traditional role in atomic spectroscopy, in photochemical studies, and in the kinetics of several of the most important visible and infrared lasers. Their role should be especially important in the extreme-ultraviolet (XUV) and soft-x-ray regions of the spectrum, where the lifetimes of nonmetastable levels are limited both by autoionization and by increasingly fast spontaneous emission.

For almost 10 years now[1] we have been developing techniques for using metastable levels for the generation of short XUV pulses, for new types of very-high-resolution core-excited spectroscopy, and for the construction of short-wavelength lasers. Our earlier efforts were based on excitation by high-power microwaves and by both cw and pulsed hollow-cathode techniques. Though sufficient to show some of the basic principles, these techniques were not sufficient to produce practical devices. About four years ago Caro et al.[2] learned how to use laser-produced x rays to produce densities of core-excited metastables that exceed 10^{15} cm^{-3}. This technique for the production of core metastables can be reasonably simple and shows promise for application in each of the above areas.

In the following sections of this paper we will review the spectroscopy of core-excited metastables, their method of production, their application to new types of ultrahigh-resolution spectroscopy, to the generation and measurement of XUV and soft-x-ray picosecond pulses, and to the construction of short-wavelength lasers.

2. SPECTROSCOPIC CONSIDERATIONS

A. Inert-Gas-Like Metastables
The paper will be concerned with two types of core-excited metastables.[3] The first are the inert-gas-like metastables that are produced by electron ionization or soft-x-ray photoionization of column I metals. The second are the class of metastable levels of alkali atoms and alkalilike ions that lie above the lowest continuum and are metastable against autoionization and sometimes against radiation.

Of these, the inert-gas-like metastables are the easiest to produce. Figure 1 shows an energy-level diagram for the production of Li$^+$(1s2s) ^1S and ^3S metastables. Soft-x-ray photons with an energy greater than 64 eV ionize a 1s electron and thereby produce the excited metastable ion; the pumping process thereby compresses broadband pumping energy into nearly monochromatic (Doppler-limited) stored energy. The population of the excited singlet or triplet ion can be determined by measuring the absorption of a laser probe beam at 958 or 549 nm, respectively.

Though the inert-gas metastables are quite easy to produce, they are difficult to invert. As was noted quite early by Hyman and co-workers,[4] the essential problem is that, when an excited ion is produced, the simultaneously produced hot electron has an energy that is more than sufficient to ionize collisionally a 2s electron, thereby producing a ground-level ion and destroying the inversion. A possible solution to this problem is to work at low ambient density, but this greatly increases the required laser pumping energy.

B. Core-Excited Doublets
To overcome the above problem, we have become interested in the class of core-excited levels that lie above the lowest continuum and are metastable against autoionization.[5] Perhaps the simplest of these are the even-parity ^2P levels of neutral Li (Fig. 2) where autoionization is prevented by the simultaneous conservation of parity and angular momentum. Table 1 shows the wavelengths and relative intensities of the transitions from this manifold.[6] The strongest of these at 20.75 nm has an Einstein A coefficient of $A = 2 \times 10^{10}$ sec^{-1}, which corresponds to a Doppler-broadened gain cross section at 700° C of 3×10^{-14} cm^2. The lower level of these transitions are valence levels of the atom that may be emptied by laser photoionization, thereby providing a four-level laser system.

C. Core-Excited Metastable Quartets
Though the core-excited Li doublets do not autoionize, they do radiate rapidly and therefore require rapid pumping. Figure 3 shows a prototype laser system[7] in which energy is
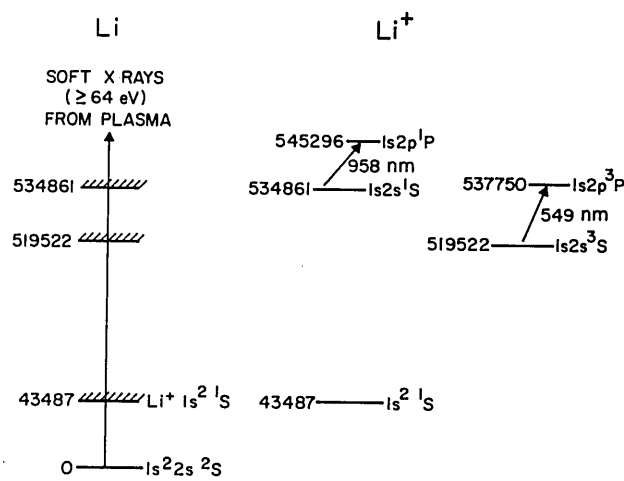
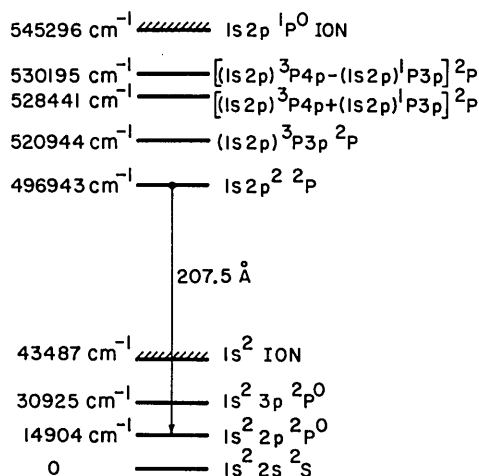Fig. 1. Energy-level diagram for producing metastable Li$^+$($1s2s$) ^1S and Li$^+$($1s2s$) ^3S ions.

Fig. 2. Energy-level diagram of neutral Li.[6]

first stored in a metastable quartet level and then transferred to a radiating doublet level by a picosecond-timescale laser pulse. Even in the heavier alkalies, quartet levels that have the highest J in a configuration have no doublet component and therefore require a spin–spin interaction to autoionize. In the absence of electrons, levels of this type are metastable for many microseconds.

There are, however, two problems associated with the Li system of Fig. 3. The first is the small intercombination oscillator strength ($f = 2.5 \times 10^{-8}$) on the 295-nm quartet-doublet transition, and the second is the need to empty the resonance level of the atom. These problems may be overcome by using heavier alkalies such as Na and K, for which the intercombination oscillator strengths are about 4 orders of magnitude greater than in Li, and for which the lower level of the laser transition is closer to the valence continuum.[8]

D. Quasi-Metastable Quartets

We have recently found that there is a subclass of quartet levels that even in the heavier elements retain metastability against autoionization and radiate quite strongly in the XUV.[9] The distinguishing property of these quartets is that the selection rules on the spin–orbit matrix elements permit nonzero matrix elements only to doublet basis levels, which are themselves prohibited from autoionizing but are radiatively allowed. For alkali atoms, the condition for such quasi-metastability is that the level have parity and orbital angular momentum that are both odd or both even, that $|J - L| = 3/2$, and that the level not be a pure (highest-J) quartet. Table 2 lists the quasi-metastable levels for the lower configurations of the alkalilike atoms that obey this selection rule.[9] Note, however, that this selection rule is weak and holds best for lower levels such as $^4S_{3/2}$ and $^4P_{5/2}$, which have the greatest energy separation from their neighbors and, therefore, have the weakest second-order coupling to autoionizing doublets.

Figure 4 shows an energy-level diagram for the 109.1-nm transition in neutral Cs. Figure 5 shows the emission spec-

Table 1. Transitions from Core-Excited ^2P States in Neutral Li

| Transition	Relative Intensity[a]	Observed Wavelength[a] (nm ± 0.01)	Calculated Wavelength[b] (nm)
$1s2p^2\,{}^2P \rightarrow 1s^22p\,{}^2P^o$	62	20.75	20.745
$\rightarrow 1s^23p\,{}^2P^o$	12	21.46	21.458
$\rightarrow 1s^24p\,{}^2P^o$	6	21.71	21.716
$\rightarrow 1s^25p\,{}^2P^o$	2	21.84	21.837
$\rightarrow 1s^2\,{}^1S + e^-$		22.05	
$(1s2p)\,{}^3P\,3p\,{}^2P \rightarrow 1s^22p\,{}^2P^o$	8	19.78	19.761
$[(1s2p)\,{}^3P\,4p + (1s2p)\,{}^1P\,3p]\,{}^2P \rightarrow 1s^22p\,{}^2P^o$	3	19.48	19.472
$\rightarrow 1s^23p\,{}^2P^o$	10	20.10	20.099
$\rightarrow 1s^24p\,{}^2P^o$	0.3	20.33	20.326
$\rightarrow 1s^25p\,{}^2P^o$	0.2	20.43	20.432
$[(1s2p)\,{}^3P\,4p - (1s2p)\,{}^1P\,3p]\,{}^2P \rightarrow 1s^23p\,{}^2P^o$	8	20.03	20.029
$\rightarrow 1s^24p\,{}^2P^o$	1.5	20.25	20.254

[a] Ref. 6.
[b] Ref. 34.
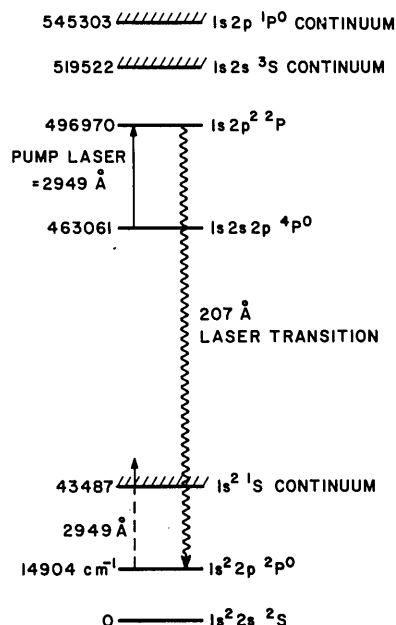
Fig. 3. Energy-level diagram for a possible 207-Å laser in neutral Li.[7]

Table 2. Quasi-Metastable and Metastable Quartet Levels of Alkalilike Configurations

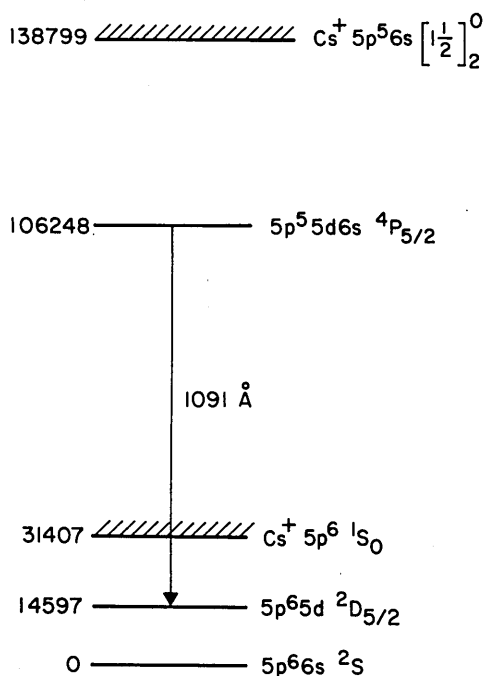| Configuration	Quasi-Metastable	Metastable
p^5sp	$^4S_{3/2}\ ^4D_{1/2}$	$^4D_{7/2}$
p^5sd	$^4P_{5/2}\ ^4F_{3/2}$	$^4F_{9/2}$
p^5pd	$^4S_{3/2}\ ^4D_{1/2}\ ^4D_{7/2}\ ^4G_{5/2}$	$^4G_{11/2}$
p^5d^2	$^4P_{5/2}$	
p^5d^2	$^4P_{5/2}\ ^4F_{3/2}\ ^4F_{9/2}$	

Fig. 4. Energy-level diagram for quasi-metastable emission in neutral Cs.[10]

trum of neutral Cs taken in a pulsed hollow-cathode discharge by Holmgren *et al.*[10] As is the case in each of the alkali atoms, the emission from the quasi-metastable levels dominates the neutral emission spectrum.[11] Table 3 gives the radiative and autoionizing rates for the lowest quasi-metastable level of each of the alkali atoms. Table 4 gives the transition wavelengths and designations of each of the quasi-metastable lines.[11]

In a recent experiment, Pedrotti *et al.*[12] have used a pulsed hollow-cathode discharge and tunable VUV radiation generated by four-wave mixing to measure the oscillator strength and hyperfine structure of the 109.1-nm transition (Fig. 4) in neutral Cs. Their value of 7.2×10^{-3} is in good agreement with the value predicted by the RCN/RCG atomic physics code.[13]

Because of their large doublet component, the quasi-metastable levels permit quartet–doublet transfer schemes at large intercombination oscillator strength and may also allow direct lasing in the XUV. As will be discussed in Section 5, they also permit a new type of core-excited laser spectroscopy.

3. PRODUCTION AND MEASUREMENT OF METASTABLES

A. Metastable Production by Microwaves

During the course of this program, we have used three methods to produce metastable atoms and ions. These are high-power microwaves, pulsed hollow-cathode discharges, and photoionization by laser-produced x rays. The microwave method is simple, and the repetition rate of 400 Hz is especially well suited for observing emission spectra at relatively low atom density (about 10^{14} cm^{-3}). Under typical conditions, about 300 kW of 9.4-GHz radiation in a 2-μsec pulse is applied to a ridged waveguide emission cell. In apparatus of
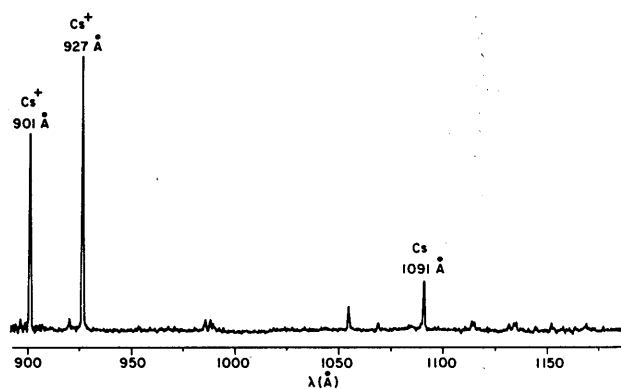

Fig. 5. Emission scan of Cs from pulsed hollow-cathode discharge.

Table 3. Radiative and Autoionizing Rates for the Lowest Quasi-Metastable Levels of the Alkali Metals

Level	Autoionizing Rate (sec^{-1})	Radiative Rate (sec^{-1})
Na $2p^53s3p\ ^4S_{3/2}$	6.8×10^5	9.7×10^6
K $3p^53d4s\ ^4P_{5/2}$	1.8×10^5	3.5×10^6
Rb $4p^55s5p\ ^4S_{3/2}$	8.5×10^7	2.6×10^7
Cs $5p^55d6s\ ^4P_{5/2}$	1.0×10^8	5.4×10^7

Table 4.   Quasi-Metastable Lines Observed with Microwave Excitation[a]

| Element	Transition	λ (nm)	Relative Intensity	Upper-Level Energy (cm^{-1})
Na	$2p^53s3p\ ^4S_{3/2} \rightarrow 2p^63p\ ^2P_{3/2,1/2}$	40.52	7.0	$263\,789 \pm 120$
K	$3p^54s4p\ ^4S_{3/2} \rightarrow 3p^64p\ ^2P_{3/2}$	67.39	23.0	$161\,426 \pm 60$
	$\rightarrow 3p^64p\ ^2P_{1/2}$	67.36	6.0	
	$3p^53d4s\ ^4F_{3/2} \rightarrow 3p^63d\ ^2D_{3/2,5/2}$	69.17	2.0	$166\,092 \pm 60$
	$3p^53d4s\ ^4P_{5/2} \rightarrow 3p^63d\ ^2D_{3/2,5/2}$	72.10	27.0	$160\,227 \pm 60$
Rb	$4p^55s5p\ ^4S_{3/2} \rightarrow 4p^65p\ ^2P_{3/2}$	82.37	30.0	$134\,220 \pm 40$
	$\rightarrow 4p^65p\ ^2P_{1/2}$	82.20	12.0	
	$\rightarrow 4p^66p\ ^2P_{3/2,1/2}$	90.53	0.5	
	$4p^54d5s\ ^4P_{5/2} \rightarrow 4p^64d\ ^2D_{5/2,3/2}$	85.18	6.0	$136\,756 \pm 40$
Cs	$5p^55d6s\ ^4P_{5/2} \rightarrow 5p^65d\ ^2D_{5/2}$	109.10	24.0	$106\,256 \pm 30$
	$\rightarrow 5p^65d\ ^2D_{3/2}$	108.98	2.0	
	$\rightarrow 5p^66d\ ^2D_{5/2,3/2}$	119.58	3.0	
	$\rightarrow 5p^67d\ ^2D_{5/2,3/2}$	124.72	1.0	

[a] Ref. 11.
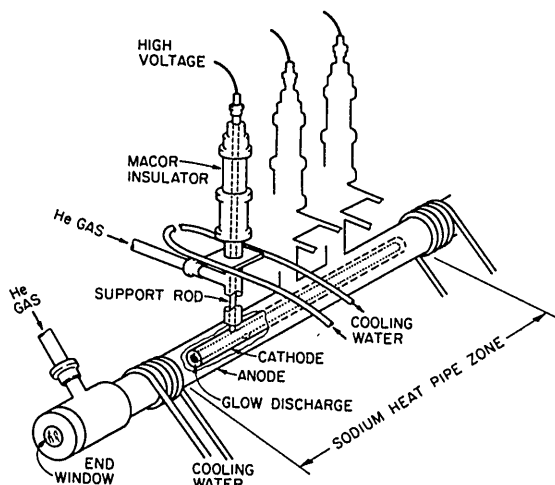
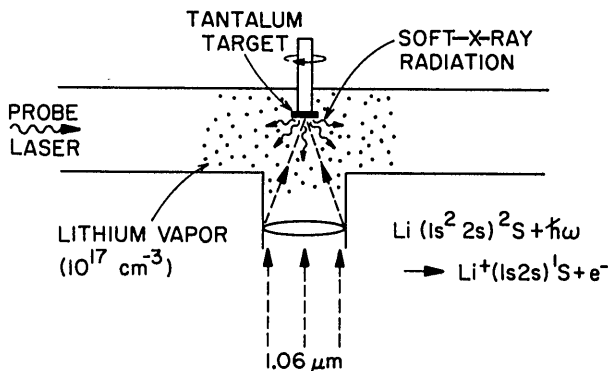Fig. 6.   Schematic of pulsed hollow-cathode discharge.[15]

Fig. 7.   Metastable production by soft x rays.

this type, electrons heat reactively; i.e., during successive half-cycles of the microwave field they first gain energy from the field and then return it to the field. For these conditions the peak reactive electron energy is about 100 eV. As electrons experience collisions with atoms and ions, they dephase with the microwave field and gain energy in increments of the reactive energy. The electron temperature is limited by electron atom and ion cooling, and by shielding of

the incoming microwaves, which occurs as the electron density rises above the plasma frequency. Willison *et al.*[6] have used this method to take the emission spectrum of the even-parity levels of Li. Mendelsohn *et al.*[11] have used it to examine the column I quasi-metastable emission spectrum, and Dimiduk[14] is now using it to study singly ionized column II quasi-metastable emission.

B.   Pulsed Hollow-Cathode Discharge

To overcome the limitations on neutral pressure of the microwave method, Falcone and co-workers[15] developed the pulsed hollow-cathode discharge shown schematically in Fig. 6. A 5-cm-diameter stainless-steel tube contains the metal vapor and serves as the discharge anode. Inside and concentric with this tube is a 30-cm-long stainless-steel tube of 1.9-cm diameter, which functions as the cathode. The device operates in a heat-pipe mode at a vapor pressure of about 6 Torr, an applied voltage of about 5 kV, and a current of about 1500 A. The pulse length is about 1 μsec, and the discharge runs at a rate of 10 Hz. Using this type of discharge, Holmgren *et al.*[16] measured populations of the metastable $(1s2s2p)\ ^4P$ level of Li, and of the analogous $(2p^53s3p)$
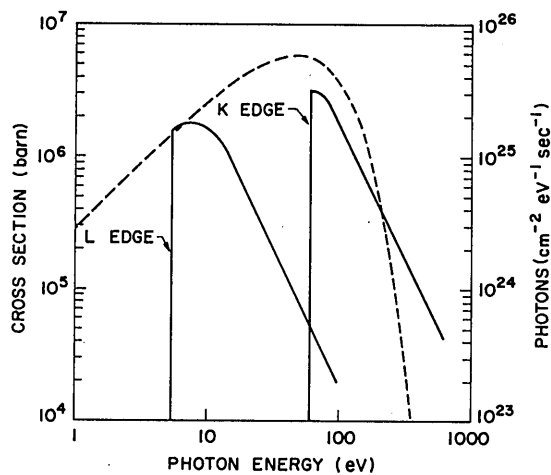

Fig. 8.   Photoionization cross sections of Li (solid curve); emission spectrum of a 30-eV blackbody (dashed curve).[22]
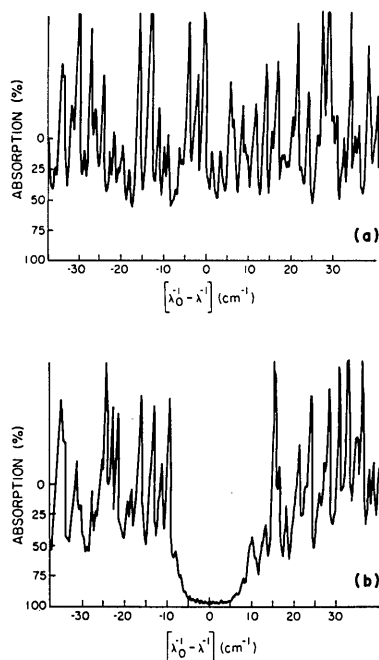
Fig. 9. (a) Spectral profile of the dye-laser probe pulse in the vicinity of 548.5 nm. (b) Absorption trace of the $Li^+(1s2s)$ ^3S–$Li^+(1s2p)$ ^3P transition at 548 nm.[23]

$^4D_{7/2}$ level of Na, of 3×10^{10} and 10^{11} cm^{-3} atoms, respectively. These populations were about a factor of 20 smaller than were those obtained in the ionic metastable levels of the same element under similar conditions. This type of discharge has also been used by Holmgren et al.[17] to obtain a partial Grotrian diagram for core-excited Na and to study quasi-metastable emission from neutral Cs.[10] Pedrotti et al.[18] used a similar technique to take the emission spectra of core-excited Na and Mg. A higher-voltage pulsed hollow-cathode discharge was also recently constructed by King and Caro.[19]

C. Metastable Production by Laser-Produced Soft X Rays

When a laser is focused onto a solid target at an intensity of 10^{12}–10^{14} W cm^{-2}, a dense plasma is formed at the surface of the target that absorbs laser radiation and is heated by it. The plasma is often black over much of the XUV and soft-x-ray region and converts laser energy to soft-x-ray energy at an efficiency that is often as high as 50%.[20] The use of such radiation to pump x-ray lasers was first suggested by Duguay[21] and was extended to the production of metastables by Hyman and co-workers.[4]

Figure 7 shows the experimental configuration that we have employed for using this radiation to produce metastable ions and atoms.[2,22] In this geometry the Li vapor surrounds the Ta target that emits the soft x rays. These x rays are omitted into about π sr and decrease in intensity as the inverse square of the distance from the target. For the construction of lasers and for many types of spectroscopic experiments, the more pertinent quantity is the product of density times perpendicular distance, which varies as the inverse of the first power of the distance from target.

Ionic metastables are produced by photoionization of core

electrons (Fig. 1). Figure 8 shows the absorption cross section as a function of soft-x-ray energy for ionization of a Li 1s or a 2s electron (1 barn = 10^{-24} cm^2) and also the spectrum of a 30-eV blackbody. For an operating pressure of 10^{17} cm^{-3}, the stopping distance for 100-eV x rays is about 10 cm. From a somewhat different point of view, a 30-eV blackbody, with an area of 10^{-3} cm^2, radiating for 1 nsec produces a spectrally integrated x-ray flux of 6.4×10^{15} photons, or 0.08 J. For the K-shell absorption cross section of Fig. 8 and a perpendicular distance from target of 0.5 cm, the spectrally integrated transition probability for a neutral atom equals
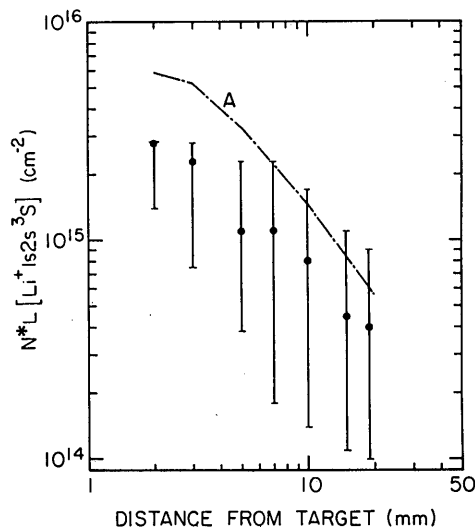

Fig. 10. N*L [$Li^+(1s2s)$ ^3S] as a function of distance from the target at a time 1.9 nsec after the peak of the 1064-nm pulse. Li density, 10^{17} cm^{-3}; energy incident upon each of three targets, 2.3 J.[23]
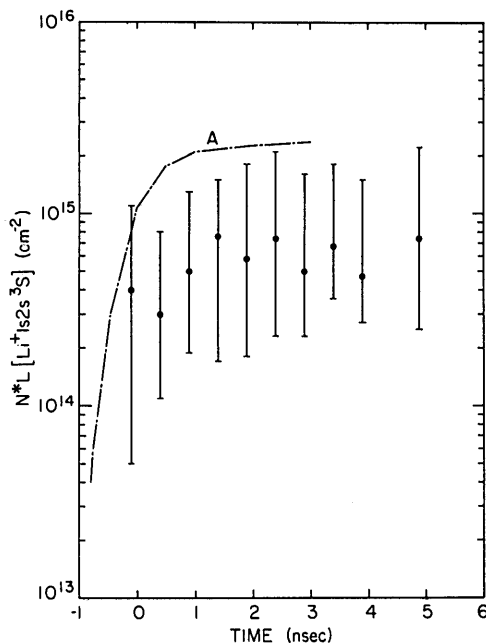

Fig. 11. N*L [$Li^+(1s2s)$ ^3S] as a function of time with respect to the peak of the 1064-nm laser pulse. Distance from targets, 7 mm; Li density, 10^{17} cm^{-3}; energy incident upon each of three targets, 2.3 J.[23]
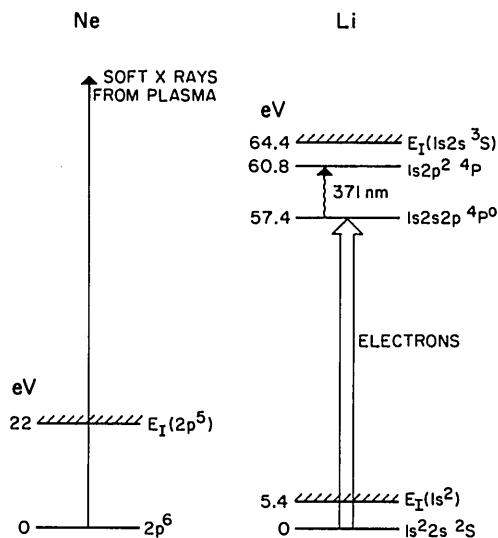
Fig. 12.   Energy-level diagram showing photoionization of the absorber atom and the subsequent electron excitation of the target atom. The laser-probe transition is also indicated.[24]

7.1×10^{-3}; i.e., for a ground-level Li density of 10^{17} cm^3, 7.1×10^{14} cm^{-3} metastable ions will be produced.

The ionic metastable density as a function of both distance and time is determined by measuring the absorption of a picosecond-time-scale probe laser tuned to an appropriate transition. For incident laser energies in the range of a joule or more, the spectral absorptions are sufficiently broad that these measurements can be made with an optical multichannel analyzer on a single-shot basis.[23] Figure 9 shows a typical absorption trace for a probe near 549 nm. The probe light for this trace was first smoothed by stimulated Rayleigh wing scattering in CS$_2$. Figures 10 and 11 show the Li$^+$(1s2s) ^3S density-times-length product obtained by Caro et al. for a three-spot target cell with 2.3 J of 1064-nm energy incident per spot, both as a function of the distance from target and as a function of time.[23] The electron density for the conditions of these figures varied between 10^{15} and 10^{16} cm^{-3}, depending on the distance from target. Even at this electron density, metastability of at least several nanoseconds is apparent.

D.   Production of X-Ray-Produced Hot Electrons

There is a second method[24] for using x rays from a laser-produced plasma for the production of metastable atoms and ions. In this method an additional absorber gas is photoionized so as to produce an impulsive burst of hot electrons. These electrons, in turn, excite core levels in the system. We have used this method to produce population in the Li(1s2s2p) ^4P level and also to measure the metastability of this level in the presence of about 10^{15} cm^{-3} electrons and ions. Figure 12 shows an energy-level diagram for this experiment, with Ne used as the additional absorber gas. Figure 13 shows the initial energy distribution of the ejected electrons for excitation with a 30-eV blackbody. At a Ne density of 10^{18} cm^{-3}, these electrons cool, primarily by excitation of the Ne resonance line, at a mean rate of about 720 eV nsec^{-1}. This allows one to use a few-hundred-picosecond probe laser, in this case at 371 nm, to measure the metastability of the target level.

Using this method, we have produced excited Li(1s2s2p) ^4P densities of 10^{13} cm^{-3}. This density is about 2 orders of

magnitude larger than that produced in our hollow cathodes but 2 orders smaller than the Li$^+$ metastable density produced by direct photoionization. Figure 14 shows the metastable times–length product density of these metastables as a function of the time delay between the 600-psec-long 1064-nm laser pulse and the probe pulse of about the same length. The observed decay time of about 2.5 nsec can be attributed to electron dipole–dipole collisional deexcitation and shows that there is not an anomalously large electron decay rate for levels that are embedded in a continuum.[24]

E.   Production by Charge Transfer

Another method by which core-excited alkali metastables may be produced is by exothermic charge transfer from the
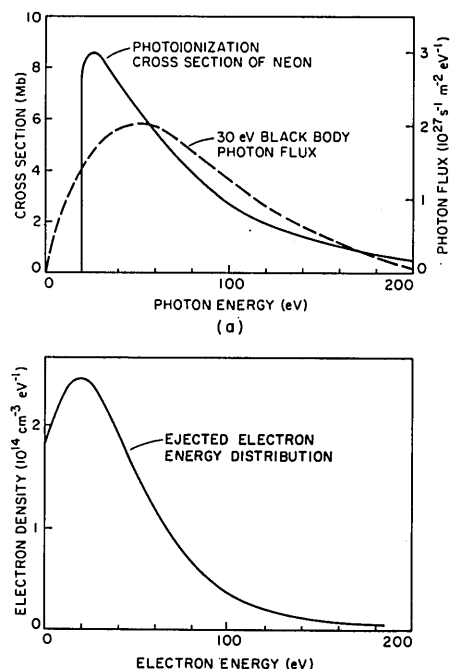

Fig. 13.   (a) Photoionization cross section of Ne and the x-ray spectrum 1 mm from the target. (b) Predicted ejected electron distribution for a Ne density of 3×10^{17} cm^{-3}.[24]

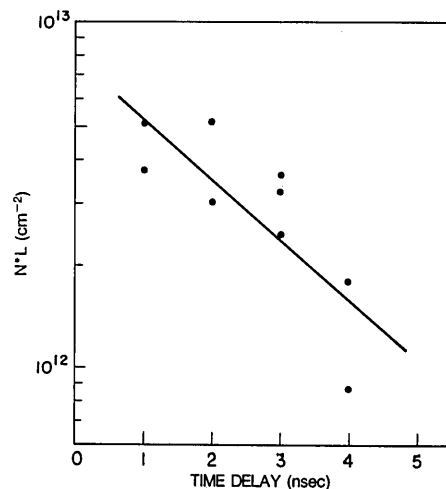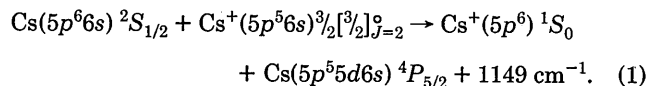Fig. 14.   N*L for Li(1s2s2p) $^4P^\circ$ versus the time delay between the peaks of the probe and 1064-nm pulses. The solid line is a fit to the data yielding $\tau_{decay} = 2.5$ nsec.[24]

Table 5. Metastable Production by Charge Transfer

Parent Ion	Donor	Metastable	Exothermicity (cm^{-1})
Li$^+$(1s2s) $^3S_0$	Li(1s^{2}2s) $^2S_{1/2}$	Li(1s2s2p) $^4P^o_{5/2}$	12 985
Na$^+$(2p^{5}3s)$^3\!/_2$[$^3\!/_2$]$^o_{J=2}$	Na(2p^{6}3s) $^2S_{1/2}$	Na(2p^{5}3s3p) $^4S_{3/2}$	1 139
K$^+$(3p^{5}4s)$^3\!/_2$[$^3\!/_2$]$^o_{J=2}$	K(3p^{6}4s) $^2S_{1/2}$	K(3p^{5}4s4p) $^4S_{3/2}$	1 081
Rb$^+$(4p^{5}5s)$^3\!/_2$[$^3\!/_2$]$^o_{J=1}$	Rb(4p^{6}5s) $^2S_{1/2}$	Rb(4p^{5}5s5p) $^4S_{3/2}$	650
Cs$^+$(5p^{5}6s)$^3\!/_2$[$^3\!/_2$]$^o_{J=2}$	Cs(5p^{6}6s) $^2S_{1/2}$	Cs(5p^{5}5d6s) $^4P_{3/2}$	1 149

ground neutral to the parent core-excited ion. For example, atoms in the Cs(5p^{5}5d6s) $^4P_{5/2}$ level may be produced by the reaction

$$\mathrm{Cs}(5p^66s)\ ^2S_{1/2} + \mathrm{Cs}^+(5p^56s)^3\!/_2[^3\!/_2]^o_{J=2} \rightarrow \mathrm{Cs}^+(5p^6)\ ^1S_0$$

$$+ \mathrm{Cs}(5p^55d6s)\ ^4P_{5/2} + 1149\ \mathrm{cm}^{-1}. \quad (1)$$

For a typical charge-transfer cross section of about 10^{-15} cm^2, and a neutral Cs density of 10^{17} cm^{-3}, about 5% of the core-excited parent ions would transfer to this level in 10 nsec. Since core-excited parent densities in excess of 10^{15} cm^{-3} are readily obtainable by x-ray photoionization, it is expected that this method should produce densities greater than 10^{13} atoms cm^{-3}.

Table 5 lists the exothermicity for charge transfer between the core-excited parents and some of the metastable levels and quasi-metastable levels of the alkali atoms. In both Na and Rb we have some early evidence that charge transfer is the operative populating mechanism. In Na, Holmgren et al.[17] note enhancement of fluorescence from neutral core levels when population is transferred to higher ion levels. In Rb, Spong et al.[25] note reduction in the quasi-metastable radiation at 82.4 nm when the Rb$^+$ level is depleted by a tunable laser.

4. GENERATION AND MEASUREMENT OF PICOSECOND PULSES

A. Generation
One of the applications of stored metastable energy is to the generation of short pulses of XUV and soft-x-ray radiation. This is accomplished by anti-Stokes scattering of picosecond-time-scale visible or ultraviolet laser pulses off metastable atoms.[26] Figure 15 shows an energy-level diagram for such scattering in He-like carbon. In this case near-UV radiation at 354.7 nm will scatter into 4.03-nm radiation. This scattering will be either stimulated or spontaneous, depending on whether the metastable atoms are, or are not, inverted with respect to ground. The cross section for spontaneous anti-Stokes scattering, i.e., the ratio of scattered XUV photons to incident laser photons, varies as the inverse square of the detuning from resonance and, at fixed XUV oscillator strength and detuning, varies as ω^3. For scattering of 354.7-nm radiation to 4.03 nm in C V, the detuning from resonance is 168 cm^{-1}, and the spontaneous anti-Stokes scattering cross section for the incident laser beam is 5.5×10^{-19} cm^2.

A limitation on the intensity of this type of radiator is posed by its nature as a two-photon blackbody.[26] This is perhaps easiest seen by describing the process in terms of a laser-induced per-atom emission rate, $A(\omega)$, and a laser-induced cross section for the absorption of XUV radiation, $\sigma(\omega)$. That is, the incident laser beam not only causes the

metastable atoms to couple through virtual levels to emit XUV radiation but also causes ground-level atoms to absorb radiation by coupling through these same virtual levels. Both $A(\omega)$ and $\sigma(\omega)$ increase linearly with incident laser intensity and are related to each other in the same manner as are the emission and absorption coefficients for single-photon processes, i.e.,

$$\sigma(\omega) = \frac{\pi^2 c^2}{\omega^2} A(\omega).$$

The brightness of the radiation source $B(\omega)$ (power per bandwidth in radians/second per solid angle) and area is determined by the interplay of the emissive and absorptive processes and, for a sample of a length L, is given by

$$B(\omega) = \frac{\hbar\omega^3}{8\pi^3 c^2}\left[\exp(\hbar\omega_{21}/kT) - 1\right]^{-1}$$

$$\times \{1 - \exp[-\sigma(\omega)(N_1 - N_2)L]\},$$

$$\sigma(\omega) = \frac{\pi\omega}{6c^2\epsilon_0^2\hbar^3}\left[\sum_i\left(\frac{\mu_{2i}\mu_{i1}}{\omega_i - \omega} + \frac{\mu_{2i}\mu_{i1}}{\omega_i + \omega_{\mathrm{vis}}}\right)\right]^2 \frac{P_p}{A} g(\omega) \quad (2)$$

(MKS units). In this expression, T is the equivalent temperature of the metastable level, i.e., $N_2/N_1 = \exp(-\hbar\omega_{21}/kT)$; μ_{ij} are matrix elements; ω_i are the frequencies of the intermediate levels; P_p/A and ω_{vis} are the intensity and frequency of the pump laser; ω is the frequency of the scattered radiation; and $g(\omega)$ is the line shape for the two-photon absorptive process.

In the optically thin case, $\sigma(\omega)(N_1 - N_2)L \ll 1$, $B(\omega)$ increases linearly with the incident laser power density and is the same as obtained from the spontaneous-scattering viewpoint of the preceding paragraph. As the laser power density is increased and the medium becomes nominally two-photon opaque, the brightness approaches a constant
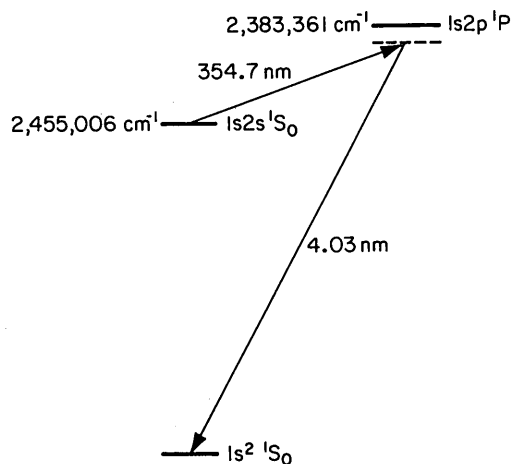

2,383,361 cm^{-1} ———— 1s2p ^{1}P

354.7 nm

2,455,006 cm^{-1} ———— 1s2s ^{1}S$_0$

4.03 nm

———— 1s^2 ^{1}S$_0$

Fig. 15. Anti-Stokes scattering in C V.

Table 6.   Anti-Stokes Scattering at Soft-X-Ray Wavelengths[a]

Species	$1s2s\ {}^1S$ (cm^{-1})	$1s2p\ {}^1P$ (cm^{-1})	$\lambda(2s \rightarrow 2p)$ (nm)	$\lambda(2p \rightarrow 1s)$ (nm)
He I	166 277	171 135	2,058.7	58.43339
Li II	491 372	501 806	958.4	19.9280
Be III	981 175	997 454	614.3	10.02552
B IV	*1 635 752*	1 657 979	*449.9*	6.03144
C V	*2 455 006*	2 483 367	352.6	4.02679
N VI	*3 439 390*	3 473 790	290.7	2.8787
O VII	*4 588 500*	4 629 090	245.7	2.16020
F VIII	*1 228 460*	5 949 900	*211.8*	1.6807
Ne IX	*7 382 890*	7 436 600	*185.2*	1.3447

[a] Experimental values are from Ref. 44; theoretical results, *in italics*, are from Ref. 45.
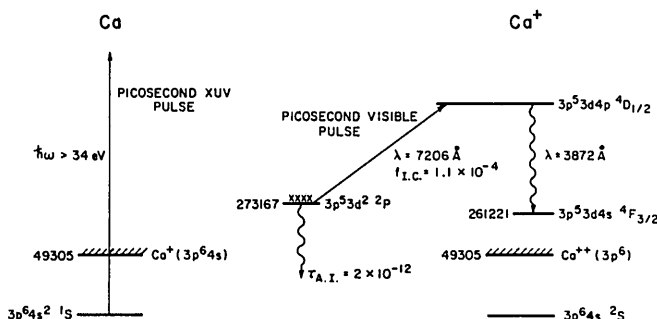

Fig. 16.   Correlation of picosecond XUV pulses.

value equal to that of a blackbody radiator at the temperature T of the metastable level. In general, and especially at short wavelengths, the temperature of the metastable level will be much higher than that of a radiating level.

Although the maximum power per bandwidth is determined by the ratio of metastables to ground-level atoms, the total emitted power may be increased by using a broadband pump laser to increase the spectral range of two-photon opacity.

In an experiment in 1978, Zych et al.[26] used a He–Ne glow discharge and a 100-psec-long pulse of 1064-nm radiation to verify the two-photon blackbody nature of the source. In that experiment they found a per-bandwidth intensity ratio of laser-induced 56.9-nm light to He resonance-line 58.4-nm light of 140.

We believe that it may be possible to use soft-x-ray photoionization to produce quite high densities of He-like metastable ions through species as high as Ne IX. For these species the necessary laser wavelength to reach the XUV resonance transition is within the range of frequency-doubled dye lasers, and the generated wavelength is as short as 1.3 nm (Table 6).

The reason why it may be possible to produce a relatively high density of a particular species is that, as an element is stripped down, the energy that is necessary for photoionization rises abruptly as the He-like species is encountered. For example, the successive ionization potentials for C are 11.3, 24.4, 47.9, 64.5, and 392.1 eV. Therefore, for a correctly chosen radiation flux and temperature, the ambient atoms will be stripped to predominantly He- and Li-like ions. Inner-shell photoionozation of the latter species will then produce the desired metastable.

For the generated XUV pulse to be as short as the incident laser pulse, it will be necessary for the detuning from the resonance line to be large compared with the bandwidth of the pulse. For the 168-cm^{-1} detuning of 354.7 nm in C V, this would permit generation of pulses as short as about 0.03 psec. For this detuning, the laser saturation energy at which $1/\epsilon$ of the stored metastable energy will be scattered is 0.34 J cm^{-2}. At a metastable density of 10^{14} cm^{-3} ions about 10^{11} photons will be scattered from a 1-mm^3 volume into 4π sr. If this occurs in 1 psec, the scattered power will be about 4.9 MW. This radiation will come from a small enough region that grazing-incidence optics, such as those discussed in Subsection 6.C, may be used to focus it into a reasonably collimated beam.

B.   Measurement

Metastable levels may also bear on the measurement of the length of picosecond-time-scale soft-x-ray pulses.[27] One approach is shown schematically in Fig. 16. Here, broadband XUV radiation with photon energy greater than 34 eV photoionizes neutral Ca and, because of configuration mixing, produces Ca II ions in the $3p^53d^2\ {}^2P$ level. These ions autoionize in about 2 psec. A picosecond-tunable laser will transfer these ions to a radiating quasi-metastable level only when the broadband XUV pulse and the tunable laser pulse overlap in time. The system, therefore, provides a means to correlate XUV pulses with optical pulses, with the minimum correlation time determined by the autoionizing time of the ion. For appropriate levels, this time may be as short as 10^{-14} sec. Note that the energies of the levels in Fig. 16 are RCN/RGN code values[13] and have not been experimentally determined.

5.   SPECTROSCOPIC APPLICATION

Over the past several years we have developed three spectroscopic techniques that are based on core-excited metastables. These new methods allow one to obtain level positions and autoionizing linewidths to the accuracy of visible lasers and, therefore, at a resolution that is about 10 times greater than that previously obtainable.

A.   Anti-Stokes Radiation Source

The first of these techniques is absorption spectroscopy using the anti-Stokes source that was described in Section 4. Metastable atoms are produced, and a tunable visible laser is scattered off these atoms to produce tunable XUV radiation that is incident upon the sample cell. The linewidth of the tunable radiation is the wider of the Doppler width of the metastable transition or the linewidth of the incident laser. In two related sets of experiments using this source Rothenberg et al.[28,29] examined a portion of the core-excited spectrum of neutral K. Figure 17 shows the apparatus used in the first of these experiments. A tunable laser is scattered off He metastables produced in a cw hollow-cathode discharge. The tunable spontaneous radiation counterpropagates through a K cell and, after passing through an Al filter, is incident onto a photomultiplier. The spontaneous anti-Stokes scattering cross section for visible photons at 600 nm to XUV photons in the 50-nm spectral region is 4×10^{-23} cm^2. For typical conditions this resulted in the generation of about 10^8 XUV photons. The available solid angle of the
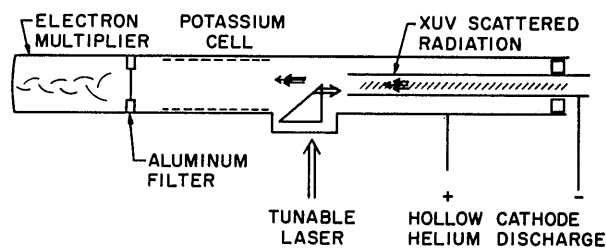
Fig. 17.   Schematic of apparatus used for absorption spectroscopy of K.[28]

detector and the Al filter reduced the effective count rate to about 800 photons per pulse, or 8,000 photons per second.

Figure 18 shows the result of a typical absorption scan. Table 7 summarizes the spectral information that was obtained.[28]   A second set of experiments used high-power-pulsed microwaves for the production of the He metastables.[29]   This produced an anti-Stokes signal that was much stronger than was the case with the pulsed hollow-cathode but also resulted in a high level of spurious XUV radiation. A spectrometer was used to reject this radiation; this in turn resulted in a net count rate that was only about a factor of 10 greater than with the cw hollow-cathode.   Table 8 summarizes the spectral information that was obtained with the microwave apparatus.   The designations in both Tables 7 and 8 were obtained from the work of Mansfield.[30]

A different, more limited, experiment that used anti-Stokes radiation was the measurement of the isotopic shift of the $1s2s\ {}^1S_0$ of ^{3}He and ^{4}He.   In this experiment Falcone et al.[31] used visible fluorescence in Ne as an internal detector for 58.37-nm radiation and measured the difference in the optical parametric oscillator wavelength that was necessary to excite the Ne from metastables from ^{3}He and ^{4}He.   The

result was a measured shift of the isotopic singlet metastable levels of 7.8 ± 0.5 cm^{-1}.

B. Laser-Generated Fluorescence

The second of the techniques that have been developed makes use of laser-produced fluorescence from atoms stored in metastable levels.   Because fluorescence must be observed, the technique is most applicable to levels that autoionize sufficiently slowly to have a good fluorescence yield. In the first of these experiments Willison et al.[32] used pulsed microwaves to produce Li($1s2s2p$) ${}^4P_{5/2}$ quartets and tunable laser radiation to transfer these atoms to the Li($1s2p^2$) ${}^2P$ level.   Radiation at 20.7 nm (Fig. 3) was observed as a function of the tunable laser wavelength.   In close accord to the predictions of Bunge[33,34] and Jáuregui and Bunge,[35] this transition was found to be at $33\ 872 \pm 2$ cm^{-1}, thus providing the first experimental connection between the quartet and doublet manifolds of neutral Li.   This technique may be

Table 7. Potassium Absorption Features

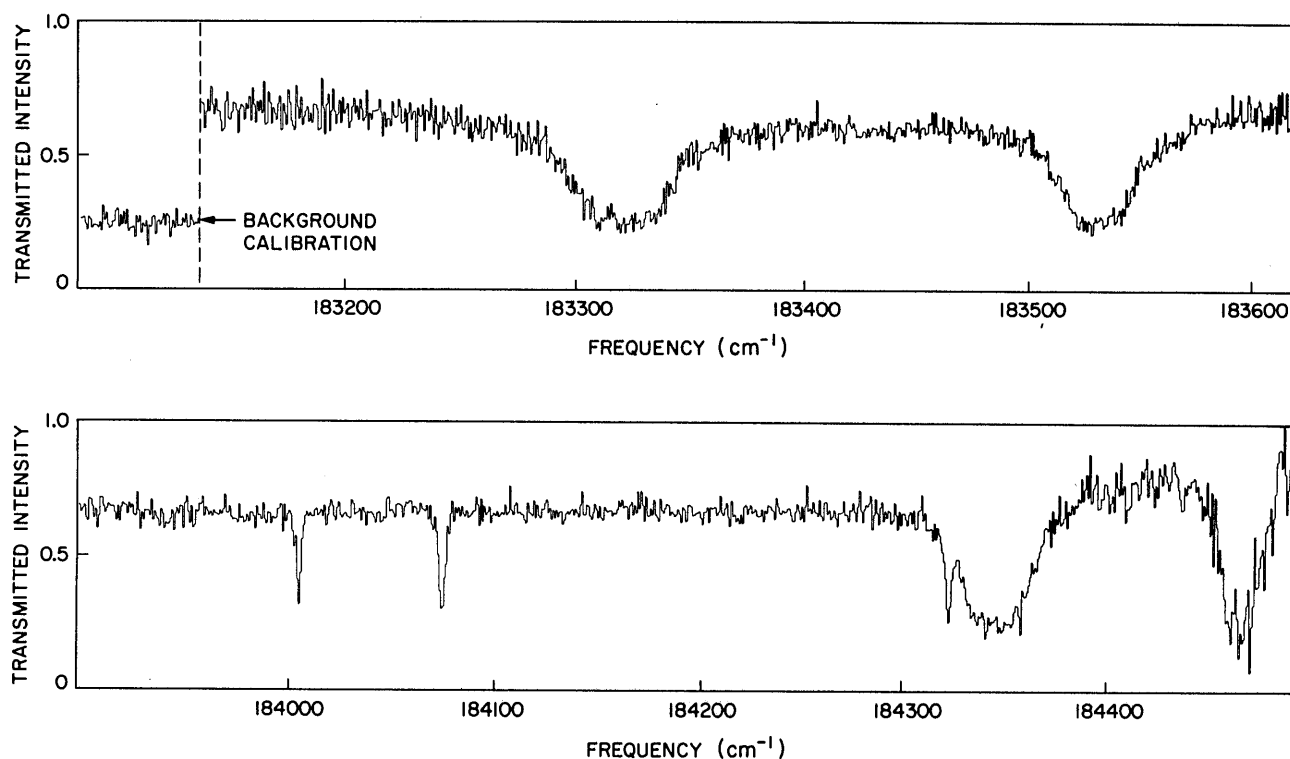| Energy	Linewidth	Designation	Previously Observed Energy[a]
$183\ 320 \pm 1$ cm^{-1}	8.4 cm^{-1}	$3p^53d({}^3P)5s\ {}^2P_{1/2}$	183 322 cm^{-1}
183 530	10.5	$3p^53d({}^3P)5s\ {}^2P_{3/2}$	183 532
184 008	2.6		
184 076	3.4		184 076
184 321	2.5		
184 344	15.0	$3p^54s({}^1P)5s\ {}^2P_{3/2}$	184 342
184 465	7.8		
185 806	1.9		
186 659	5.0	$3p^54d({}^1D)4s\ {}^2D_{3/2}$	186 656

[a] Ref. 28.

Fig. 18.   Absorption scans of K.   Vapor pressure is 10^{15} cm^{-3}, and cell length is 5 cm.[28]

Table 8. Linewidths and Positions of Potassium Absorption Features Observed with the Microwave Apparatus

Energy (cm^{-1})	Linewidth (cm^{-1})	Designation	Previously Observed Energy (cm^{-1})[a]
179 885	4.0	$3p^53d(^3D)4s\ ^2D^0_{3/2}$	179 886
179 918	2.1		179 920
180 547	43.0	$3p^53d(^1P)4s\ ^2P^0_{1/2}$	180 551
180 794	55.0	$3p^55d(^1P)4s\ ^2P^0_{3/2}$	180 791
180 840	11.0		180 850
181 519	2.7		181 517
181 745	5.5	$3p^53d5s\ ^4P^0_{3/2}$	181 742
182 152	8.8		182 152
182 652	5.6		182 651

[a] Ref. 29.

used for transitions that have very small oscillator strengths. For example, for the $1s2s2p\ ^4P \to 1s2p^2\ ^2P$ transition, with an oscillator strength of 2.5×10^{-8}, 36% of the population within the 0.2-mm^2 beam was transferred with 10 mJ of laser energy.

Using a related method, Holmgren et al.[17] used metastable population to develop a partial Grotrian diagram for core-excited Na. In this experiment a pulsed hollow cathode was used to excite the metastable $2p^53s3p\ ^4D_{7/2}$ and the $2p^53s3p\ ^4S_{3/2}$ quasi-metastable levels, and a tunable laser was used to transfer this population to other core-excited levels. Visible and near-UV fluorescence from these latter levels was observed, and loops were established between interconnected levels. Branching ratios were also measured and found to agree to within a factor of 3.5 with calculated

values based on the RCN/RCG atomic physics code.[13] Recently, Engström et al.[36] have given further confirmation of these ratios. Tables 9 and 10 summarize the results of Holmgren et al., and Fig. 19 shows the brighter lines of the Na spectrum.

C. Laser-Depletion Spectroscopy

In quite recent work Spong et al.[25] have demonstrated what may be the most powerful of the laser spectroscopic methods. In this technique the XUV radiation from a quasi-metastable level is monitored, and a tunable laser is scanned over the region where other autoionizing lines are expected to be present. When one is encountered, the quasi-metastable radiation is depleted, thereby determining its autoionizing linewidth and its position relative to the quasi-metastable level. By using a curve-fitting method, which is in one-to-one correspondence with the curve-of-growth method, the transition oscillator strength may also be determined.

In this work the $4p^55s5p\ ^4S_{3/2}$ quasi-metastable level of Rb is excited by laser-produced x rays (Fig. 20), and radiation at 82.4 nm is monitored with a wide-slit spectrometer. Table 11 gives the linewidth, transition energy, and tentative designations of the depletion transitions that we have thus far observed. These first results give linewidths, and therefore autoionizing times, to an accuracy that is at least 20 times greater than given previously.

In an earlier experiment, using pulsed hollow-cathode technology, Pedrotti[37] observed radiation at 20.7 nm in Li and used this depletion technique to obtain a width of 25.5 cm^{-1} for the Li $1s(2s2p\ ^3P)\ ^2P$ autoionizing line at 475 163 cm^{-1}.

By observing the radiation from an appropriate quasi-metastable level, this technique permits observation of autoionizing lines of both even and odd parity and with J values that make them inaccessible by optical absorption from ground. The observation of Rydberg transitions and interferences should also be possible.

Table 9. Relative Term Energies, Designations, and Coulombic Autoionizing Rates of Na I Core-Excited Quartet Levels

Configuration	Energy (cm^{-1})[a]	Composition	Autoionizing Rate (sec^{-1})
$2p^53s3p$	0	$0.98\ ^4S_{3/2} - 0.13\ ^4P_{3/2}$	4.15×10^5
	2 841	$0.99\ ^4D_{7/2}$	0
	3 187	$0.94\ ^4D_{5/2} - 0.21\ ^4P_{5/2} + 0.18(^1P)\ ^2D_{5/2}$	1.25×10^{10}
	3 536	$-0.92\ ^4D_{3/2} + 0.23\ ^4P_{3/2} - 0.22(^1P)\ ^2D_{3/2}$	1.79×10^{10}
	3 830	$-0.94\ ^4D_{1/2} + 0.22(^1P)\ ^2P_{1/2} + 0.20\ ^4P_{1/2}$	1.06×10^9
	4 768	$0.91\ ^4P_{5/2} + 0.32(^1P)\ ^2D_{5/2} + 0.20(^3P)\ ^2D_{5/2}$	3.84×10^{10}
	5 152	$0.76\ ^4P_{3/2} + 0.48(^1P)\ ^2D_{3/2} + 0.30(^3P)\ ^2D_{3/2}$ $+ 0.22(^1P)\ ^2P_{3/2}$	8.59×10^{10}
$2p^53s4s$	22 555	$-1.0\ ^4P_{5/2}$	2.93×10^{-3}
$2p^53s3d$	28 474	$0.97\ ^4P_{1/2} - 0.24\ ^4D_{1/2}$	2.02×10^6
	28 543	$0.86\ ^4P_{3/2} - 0.49\ ^4D_{3/2}$	1.76×10^8
	28 595	$-1.0\ ^4F_{9/2}$	0
	28 654	$0.72\ ^4D_{5/2} - 0.60\ ^4P_{5/2} - 0.33\ ^4F_{5/2}$	1.02×10^6
	28 703	$0.71\ ^4F_{7/2} - 0.70\ ^4D_{7/2}$	1.76×10^8
	29 168	$-0.73\ ^4F_{5/2} + 0.58\ ^4P_{5/2} + 0.26(^1P)\ ^2D_{5/2}$	5.08×10^9
	29 264	$-0.65\ ^4D_{3/2} + 0.54\ ^4F_{3/2} - 0.42\ ^4P_{3/2}$ $+ 0.22(^1P)\ ^2P_{3/2} - 0.21(^1P)\ ^2D_{3/2}$	1.55×10^9

[a] ± 2 cm^{-1}.

Table 10.   Na I Quartet Transition Wavelengths, Transitions, Probabilities, Branching Ratios (B · R), and Observed Line Intensities

Upper Level	Lower Level	λ (Å)[a]	A_{ik} (10^8 sec^{-1})	g_iB · R	Experimental Intensity
$(2p^53s3d)\,^4P_{1/2}$	$(2p^53s3p)\,^4S_{3/2}$	3511.0	1.15	1.3	1.3
	$^4P_{3/2}$	4286.7	0.28	0.32	0.46
	$^4D_{3/2}$	4008.8	0.15	0.18	0.27
$^4P_{3/2}$	$^4S_{3/2}$	3502.5	0.88	1.0	1.6
	$^4P_{3/2}$	4273.9	0.16	0.18	0.23
	$^4P_{5/2}$	4204.9	0.25	0.28	0.46
	$^4D_{3/2}$	3997.7	0.08	0.09	0.14
	$^4D_{5/2}$	3942.6	0.21	0.24	0.32
$^4D_{3/2}$	$^4S_{3/2}$	3416.2	0.15	0.03	
	$^4D_{1/2}$	3930.6	0.25	0.05	0.15
	$^4D_{3/2}$	3885.7	0.62	0.12	0.36
$^4D_{5/2}$	$^4S_{3/2}$	3489.0	0.42	1.5	1.3
	$^4P_{3/2}$	4253.8	0.05	0.18	0.17
	$^4P_{5/2}$	4185.5	0.49	1.8	1.5
	$^4D_{3/2}$	3980.3	0.05	0.18	0.14
	$^4D_{5/2}$	3925.6	0.45	1.6	0.85
	$^4D_{7/2}$	3872.9	0.12	0.45	0.19
$^4F_{5/2}$	$^4S_{3/2}$	3427.3	0.28	0.11	0.09
	$^4D_{5/2}$	3848.0	0.28	0.03	0.05
	$^4D_{3/2}$	3900.4	0.77	0.08	0.15
$^4F_{7/2}$	$^4P_{5/2}$	4176.7	0.35	0.83	0.82
	$^4D_{5/2}$	3917.9	0.66	1.5	1.6
	$^4D_{7/2}$	3865.5	0.58	1.4	1.3
$^4F_{9/2}$	$^4D_{7/2}$	3881.8	1.63	10.0	4.2
$(2p^53s4s)\,^4P_{5/2}$	$^4S_{3/2}$	4432.3	0.14	0.91	3.1
	$^4P_{3/2}$	5744.2	0.04	0.23	0.12
	$^4P_{5/2}$	5621.0	0.14	0.91	0.42
	$^4D_{3/2}$	5256.4	0.02	0.16	0.07
	$^4D_{5/2}$	5162.5	0.15	1.0	0.83
	$^4D_{7/2}$	5071.2	0.41	2.7	2.7

[a] Air wavelengths, ±0.2 Å.

6.   LASERS

Of the several applications of core-excited metastable levels, the application to the construction of lasers has thus far proven the most elusive.   The essential difficulty is that the inert gaslike metastables, i.e., Li$^+$(1s2s) ^1S, which we know how to produce in large densities, are difficult to invert; while on the other hand the column I metastables and quasi-metastables, which are invertable with regard to valence levels of the atom, are more difficult to produce.   The lack of knowledge of the spectroscopy of these latter species also makes population measurement difficult and forces the use of less-than-optimum systems.

A.   Power and Energy Requirements

We begin by considering the requirements on pumping power and energy for reasonably well-chosen laser systems in the 10–100-nm spectral region.   Table 12 lists the species, transition, and Doppler-limited gain cross section for several of the species that we have studied.   The table includes not only the metastable systems discussed thus far but also some systems that are based on selective Auger decay, which will be discussed somewhat further below.

Since the metastable store-and-transfer approach will not easily allow the use of resonators, lasers of this type will require a single-pass gain of about exp(20) to saturate fully.   For a gain cross section of 10^{-13} cm^2, this requires an excited density times length product of $NL = 2 \times 10^{14}$ cm^2.   By one of several approaches it should become possible to confine the pumped area to about 1 cm^2, thereby requiring a total of 2×10^{14} excited atoms.   For atoms with an energy of 100 eV, this requires a total stored energy of about 3 mJ.

We next assume that pumping occurs by photoionization by laser-produced x rays.   Though conversion efficiencies as high as 80% from laser energy to x-ray energy have been reported, 10% conversion efficiency into the useful bandwidth is more typical.   If these x rays can be completely absorbed, then in the ideal case a laser pumping energy of about 30 mJ will be required.   For the metastable store-and-transfer systems this energy can be deposited in about 1 nsec, while in direct pumped systems with large oscillator strength and, therefore, small spontaneous-emission time, it will have to be deposited in less than 100 psec.

In a realistic system there will be additional inefficiencies.   In a photoionization-pumped system, x rays are often
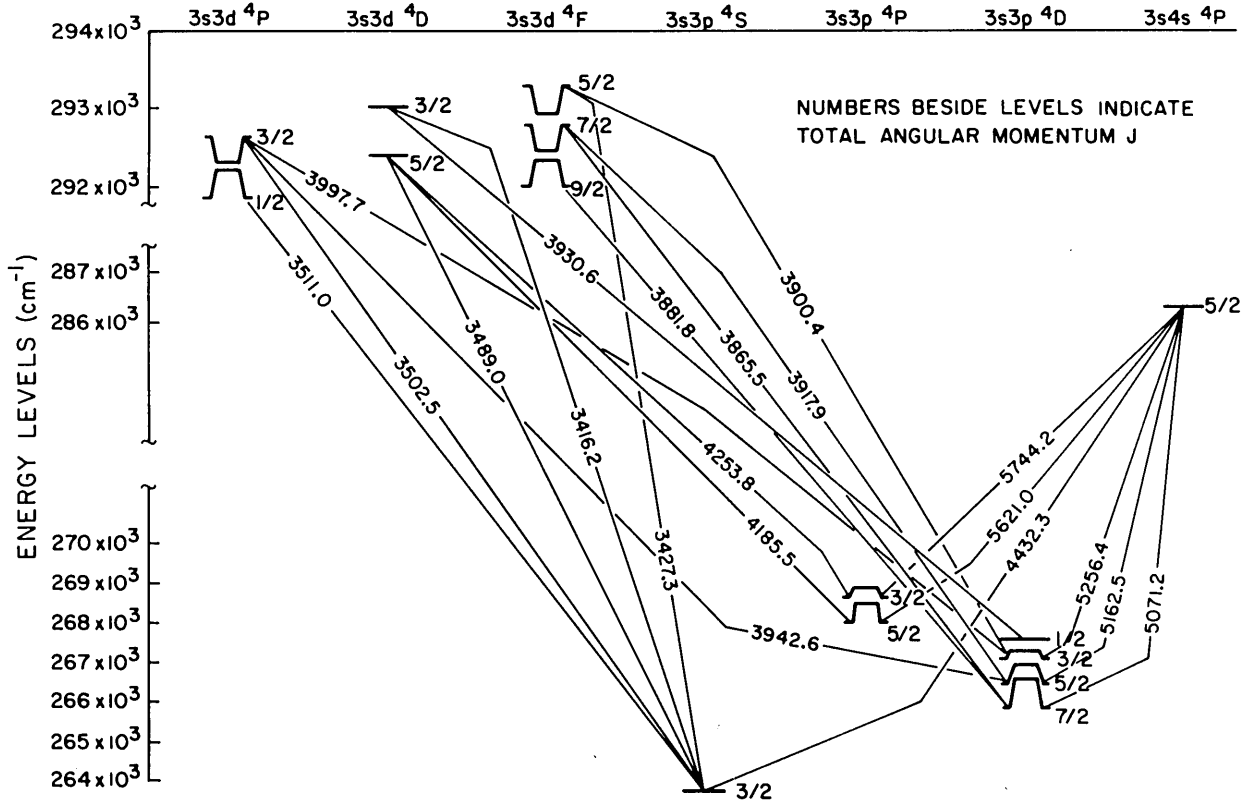
Coherent XUV and Soft Radiation

Fig. 19.   Na I core-excited Grotrian diagram.[17]
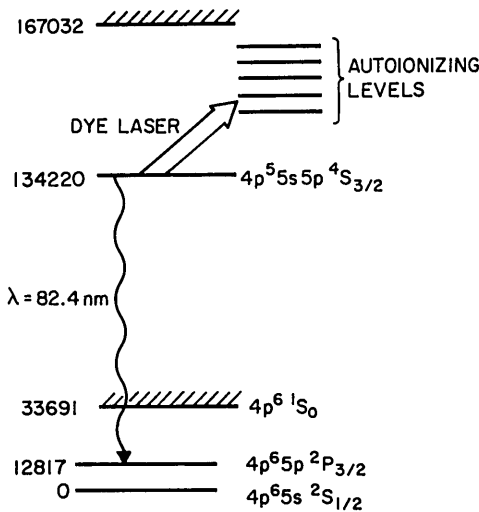
Fig. 20.   Laser depletion spectroscopy in Rb.

Table 11.   Depletion Spectroscopy of Neutral Rb

Observed Energy (cm^{-1})	Linewidth (cm^{-1})	Tentative Designation[a]	Previously Observed Energy (cm^{-1})[b]
148 874	<0.5	$4p^54d5s\ ^2D_{3/2}$	148 880
150 559	2.3	$4p^55s6s\ ^4P_{5/2}$	150 583
151 282	<0.5		
152 287	2.6		152 348
153 384	1.4		153 356
154 016	36.0	$4p^54d5s\ ^4P_{3/2}$	154 082

[a] RCN/RCG atomic physics code, Ref. 13.
[b] Ref. 46.

stopped by electrons in shells other than the desired one; in an Auger-pumped system the yields to a particular level will not often exceed 20%; in other systems pumping by secondary processes such as charge transfer will be necessary, and the efficiencies of these processes are not yet known. Even so, it appears that photoionization pumping of metastable levels offer the prospect of a class of lasers that are both efficient and have a threshold pumping energy of under a joule.

B.   Laser Systems

When possible, direct photoionization by laser-produced x rays is the preferred pumping mechanism. This approach was proposed by Duguay[21] and extended to metastable systems by Mahr and Roeder and Hyman and co-workers.[4] Using the geometry of Caro et al.,[2] Silfvast and colleagues constructed a photoionization-pumped 442-nm Cd laser[38] and also used a tunable laser to transfer population to higher levels to construct several near-UV lasers.[39]

Though direct photoionization readily leads to inversion on intermediate transitions, it is not yet clear if it may be used to produce an inversion with respect to ground. Problems include the production of ground-level ions by longer-wavelength x rays, by x-ray-produced electrons, and through autoionization.[4] By operating at much lower pressure, and by using appropriate filters, it may well be possible to overcome these problems but probably at the expense of much higher pumping energy.

Another way to use photoionization pumping is through selective Auger processes.[40–42] The potential advantage of such systems is that lasing may occur to high-lying levels in the second ion, thereby avoiding the problems of direct pho-

Table 12. Possible Laser Systems

Species	Process	λ_{LASER} (nm)	σ_{GAIN} (cm^2)
	Metastable transfer		
Li I	$1s2s2p\,^4P^\circ + \hbar\omega\,(295\text{ nm}) \rightarrow$		
	$1s2p^2\,^2P \rightarrow 1s^22p\,^2P^\circ$	20.7	9.7×10^{-14}
Na I	$2p^53s3p\,^4S_{3/2} + \hbar\omega\,(342\text{ nm}) \rightarrow$		
	$2p^53s3p\,^4D_{3/2} \rightarrow 2p^63d\,^2D_{3/2,5/2}$	37.9	6.9×10^{-15}
	Quasi-metastable		
K I	$3p^53d4s\,^4P_{5/2} \rightarrow 3p^63d\,^2D_{5/2}$	72.1	4.9×10^{-16}
Rb I	$4p^55s6p\,^4S_{3/2} \rightarrow 4p^65p\,^2P_{3/2}$	82.3	5.1×10^{-15}
Cs I	$5p^55d6s\,^4P_{5/2} \rightarrow 5p^65d\,^2D_{5/2}$	109.1	4.9×10^{-14}
	Shake-up		
Li II	$1s3s\,^3S \rightarrow 1s2p\,^3P$	165.3	1.0×10^{-13}
	Auger		
Zn III	$3d^84s^2\,^1G_4 \rightarrow 3d^94p\,^1F_3$	133.2	8.8×10^{-13}
Cs III	$5s^25p^46s\,^2D_{5/2} \rightarrow 5s^25p^5\,^2P_{3/2}$	63.8	5.6×10^{-13}
Rb III	$4s^24p^45s\,^2S_{1/2} \rightarrow 4s^24p^5\,^2P_{3/2}$	49.0	5.7×10^{-13}

toionization. One example[41] of such a system is shown in Fig. 21. Here, photoionization of a $3p$ electron in neutral Zn leads, through super-Coster–Kronig decay, to inversion of the $3p^53d^84s^2\,^1G_4$ level of Zn III with regard to several levels in the $3d^94p$ and $3d^94s$ configurations. Possible lasing transitions are shown in Fig. 22. The Einstein A coefficient of the 133.2-nm transition results from configuration mixing, and the metastability of this level is therefore uncertain. We have not yet been able to identify a selective Auger system, with good yield, to a completely metastable level.

We turn next to the metastable and quasi-metastable systems of column I. Much has been said of these systems in the previous sections. An example of a metastable transfer system in Na, which overcomes the small intercombination oscillator strength difficulty of the earlier Li system, is shown in Fig. 23. The parameters of this system, as well as those of two related systems, are shown in Table 13. In these systems it is intended to create an inversion by photoionization of the valence $3d$ electron. We are also interested in systems in which transfer would be to a Rydberg level and where, therefore, photoionization of the lower level may not be necessary. As compared with the Auger systems, these systems have the advantage that they typically have much lower loss at the lasing wavelength, and the disadvantage that, at least to date, that they are excited much less efficiently.

C. Geometry

Most of the work to date on photoionization-pumped lasers has made use of a single-spot or multispot transverse geometry (Fig. 7) in which the laser beam propagates through the ambient vapor and is incident onto a heavy metal target. The generated x rays are emitted into about π sr, and their intensity reduces as the square of the distance from the target. The NL product, which is the pertinent quantity for pumping lasers, therefore decreases linearly as the perpendicular distance. In practice, for any laser system there will be a maximum x-ray power density at which it may operate. At a given laser energy per spot, this density, or perhaps plasma blowoff, will limit the distance of closest approach to the target. If more laser energy is available, one uses multi-

ple spots or, at high enough energy, a cylindrical lens and a line focus.

As a means for obtaining additional length at a given power density, we have recently suggested[43] the alternative geometry shown in Fig. 24. Here, a section of a prolate ellipsoid is used to reflect at grazing incidence the radiation from a laser-produced plasma located at one focus to a target cell in the region of the second focus. The effective f-number and optical efficiency of this type of nonimaging optic may be very large. For example, at a wavelength of 10 nm, the grazing-incidence reflectivity of a Au surface is greater than 75% for all rays with grazing angles less than 10 deg. In the transverse plane, rays are collected over the full surface of revolution, yielding a total solid-angle collection approaching 1 sr. Figure 25 shows the fraction of collected soft x rays as a function of the ratio of the minor half-axis to the half-focal separation (b/c) for a point source placed at the first focus.

For a point source and a perfectly accurate surface, the radiation is focused into an annular cone that converges with a half-angle of about $1/2(b/c)$. For a finite source dimen-
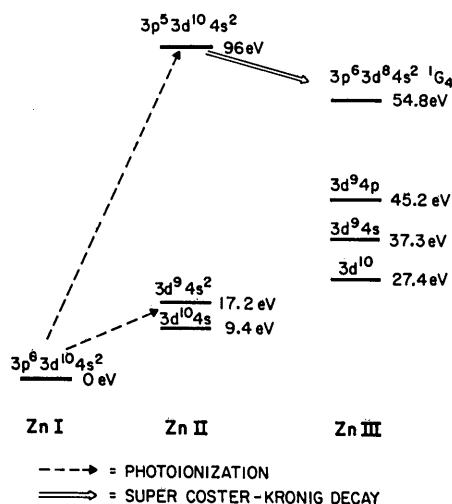

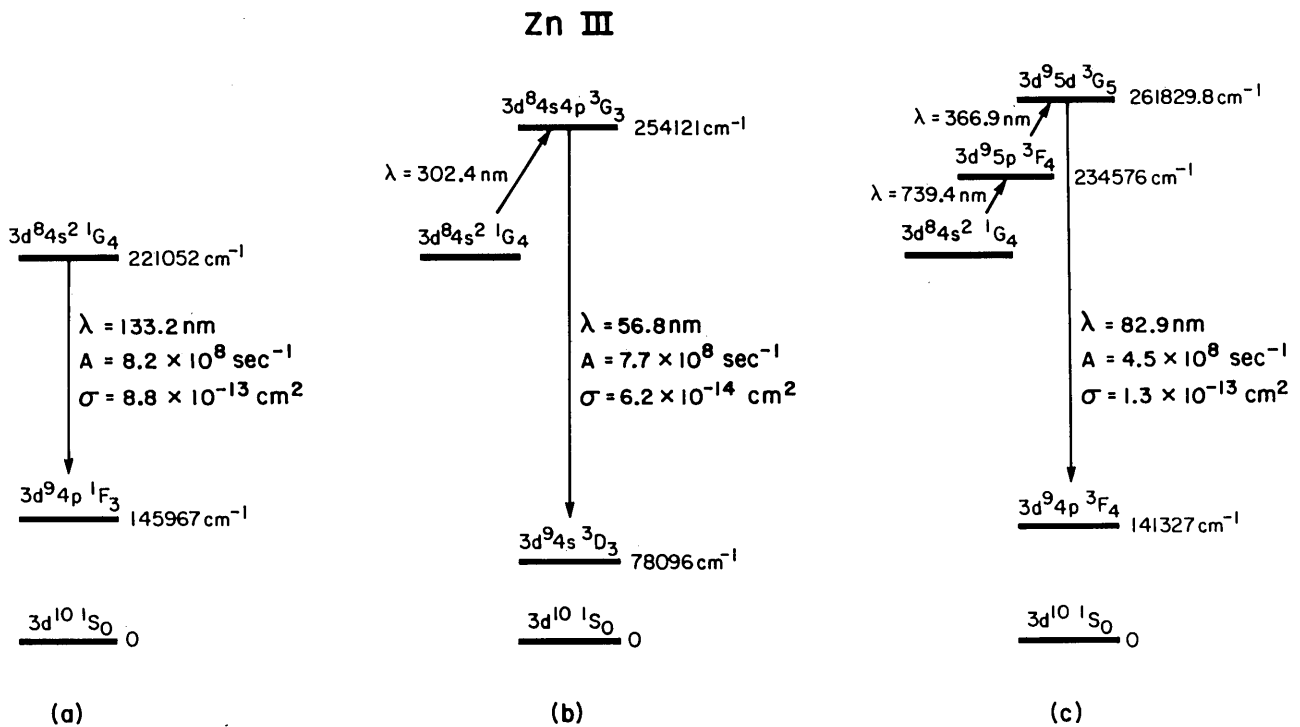Fig. 21. Population of $3d^84s^2\,^1G_4$ level by super-Coster–Kronig decay.[41]

Zn III

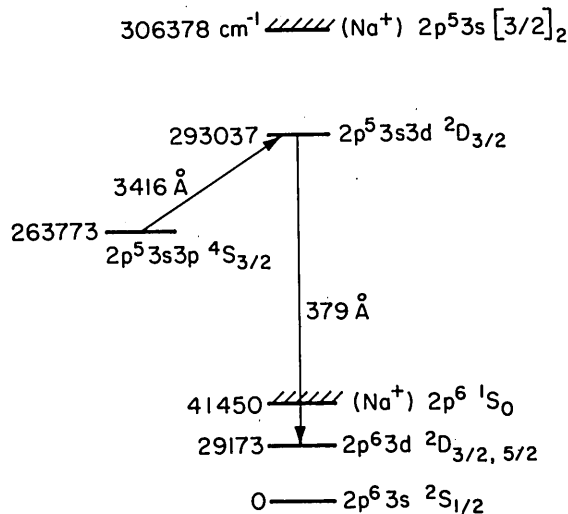Fig. 22.   Energy-level diagrams for three possible systems in Zn III.[41]

Fig. 23.   Energy-level diagram for a 379-Å laser in Na.

produce a linear magnification of the source of about 10, with an aspect ratio of approximately 25.

The comparison of the elliptical end-pumping geometry with the transverse pumping geometry is dependent on the parameters of the particular laser system. To the extent that the laser may be focused to a sufficiently small spot on target, the end-pumping geometry has a substantial power density times length, and therefore gain, advantage over the transverse pumping geometry. For example, at a 50-μm target spot size, this advantage is about a factor of 20. On the other hand, in many systems such a small spot is not able to radiate at a sufficient rate to pump the system, and in order for the available laser energy to be used maximally the
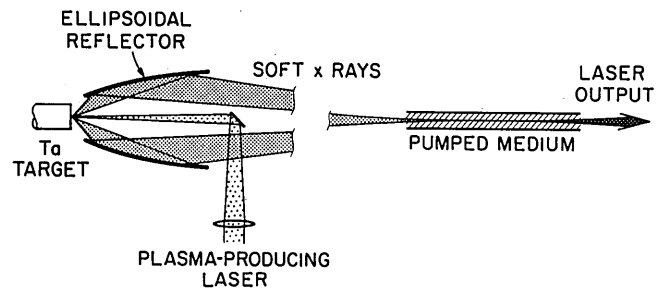
sion, the qualitative nature of the focus is determined by the conservation of optical étendue, i.e., $A_1\Omega_1 = A_2\Omega_2$, where Ω and A are solid angle and area, respectively. The solid angle Ω_1 intercepted by the short section of the eccentric ellipsoid is typically about $\pi/3$ sr, and the focal area is given approximately by $A_2 = A_1/(b/c)^2$. For a $b/c = 0.1$, the optic will

Fig. 24.   Schematic of longitudinal pumping using a prolate ellipsoidal reflector.[43]

Table 13.   Possible XUV Lasers in Na I

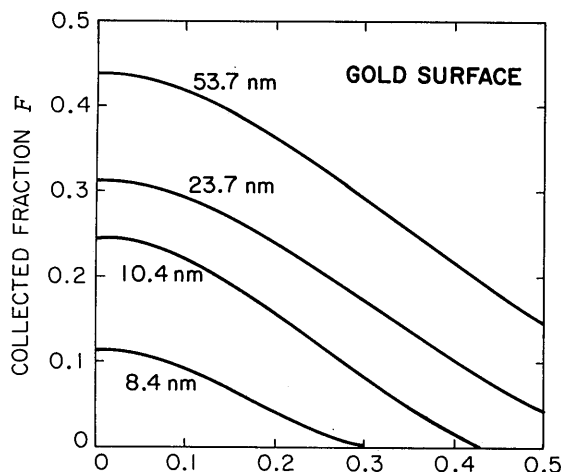| Upper Level	τ_{AI} (psec)	Transfer gf	Transfer λ (nm)	Laser gf	σ_{gain} (cm^2)	Laser λ (nm)
$2p^5 3s 3d\ ^4D_{3/2}$	645	0.10	341.6	0.038	6.9×10^{-15}	37.90
$2p^5 3s 3d\ ^4F_{5/2}$	196	0.30	342.7	0.055	6.5×10^{-15}	37.91
$2p^5 3s 3d\ ^2D_{5/2}$	45	0.011	~314	0.485	5.6×10^{-14}	37.53

Fig. 25.   Fraction F of source energy delivered to the focal plane versus ellipsoid shape; b/c is the ratio of the semiminor to the half-focal separation.[43]

target spot size must be enlarged. At a spot size of about 1 mm^2, the end-pumping and transverse geometries have about the same gain. Even here, the end-pumping geometry has the advantage of permitting a small target cell with an inherently improved aspect ratio.

ACKNOWLEDGMENTS

REFERENCES

1. S. E. Harris, "Spontaneous anti-Stokes scattering as a high-resolution and picosecond-time-scale VUV light source," Appl. Phys. Lett. **31,** 498 (1977).
2. R. G. Caro, J. C. Wang, R. W. Falcone, J. F. Young, and S. E. Harris, "Soft x-ray pumping of metastable levels of Li$^+$," Appl. Phys. Lett. **42,** 9 (1983).
3. S. E. Harris, R. G. Caro, R. W. Falcone, D. E. Holmgren, J. E. Rothenberg, D. J. Walker, J. C. Wang, J. R. Willison, and J. F. Young, "Metastability in the XUV: lasers and spectroscopy," in *Atomic Physics 9*, R. S. Van Dyck, Jr., and E. N. Fortson, eds. (World Scientific, Singapore, 1985), pp. 462–479.
4. S. A. Hyman and J. D. Daugherty, "Lithium-ion soft-x-ray laser," J. Appl. Phys. **47,** 3099 (1976); H. A. Hyman and S. A. Mani, "Effect of autoionizing states on the proposed lithium soft x-ray laser," Opt. Commun. **20,** 209 (1977).
5. P. Feldman and R. Novick, "Autoionizing states in the alkali atoms with microsecond lifetimes," Phys. Rev. Lett. **11,** 278 (1963); "Auto-ionizing states in the alkali atoms with microsecond lifetimes," Phys. Rev. **160,** 143 (1967).
6. J. R. Willison, R. W. Falcone, J. C. Wang, J. F. Young, and S. E. Harris, "Emission spectra of core-excited even-parity ^2P states of neutral lithium," Phys. Rev. Lett. **44,** 1125 (1980).
7. S. E. Harris, "Proposal for a 207-Å laser in lithium," Opt. Lett. **5,** 1 (1980).
8. J. E. Rothenberg and S. E. Harris, "XUV lasers by quartet to doublet energy transfer in alkali atoms," IEEE J. Quantum Electron. **QE-17,** 418 (1981).
9. S. E. Harris, D. J. Walker, R. G. Caro, A. J. Mendelsohn, and R. D. Cowan, "Quasi-metastable quartet levels in alkali-like atoms and ions," Opt. Lett. **9,** 168 (1984).
10. D. E. Holmgren, D. J. Walker, and S. E. Harris, "Emission at 1091 Å in neutral core-excited Cs," in *Laser Techniques in the Extreme Ultraviolet*, S. E. Harris and T. B. Lucatorto, eds. (American Institute of Physics, New York, 1984), pp. 496–501.
11. A. J. Mendelsohn, C. P. J. Barty, M. H. Sher, J. F. Young, and S. E. Harris, "Emission spectra of quasi-metastable levels of alkali atoms," Phys. Rev. A (to be published).
12. K. D. Pedrotti, D. P. Dimiduk, J. F. Young, and S. E. Harris, "Identification and oscillator strength measurement of the 109.1-nm transition in neutral Cs," Opt. Lett. **11,** 425 (1986).
13. R. D. Cowan, *The Theory of Atomic Structure and Spectra* (U. California Press, Berkeley, Calif., 1981), Secs. 8-1, 16-1, and 18-7.
14. D. P. Dimiduk, NASA Ames Research Center, Moffett Field, California 94035 (personal communication).
15. R. W. Falcone and K. D. Pedrotti, "Pulsed hollow-cathode discharge for extreme-ultraviolet lasers and radiation sources," Opt. Lett. **7,** 74 (1982); R. W. Falcone, D. E. Holmgren, and K. D. Pedrotti, "Hollow-cathode discharge for XUV lasers and radiation sources," AIP Conf. Proc. **90,** 287 (1982).
16. D. E. Holmgren, R. W. Falcone, D. J. Walker, and S. E. Harris, "Measurement of lithium and sodium metastable quartet in a hollow-cathode discharge," Opt. Lett. **9,** 85 (1984).
17. D. E. Holmgren, D. J. Walker, D. A. King, and S. E. Harris, "Laser spectroscopy of Na I quartets," Phys. Rev. A **31,** 677 (1985).
18. K. D. Pedrotti, J. J. Mendelsohn, R. W. Falcone, J. F. Young, and S. E. Harris, "Extreme-ultraviolet emission spectra of core-excited levels in sodium and magnesium," J. Opt. Soc. Am. B **2,** 1942 (1985).
19. D. A. King and R. G. Caro, "A fast, high-current pulsed discharge device for the inner-shell excitation of atoms and ions," IEEE J. Quantum Electron. (to be published).
20. K. Eidmann and T. Kishimoto, "Absolutely measured x-ray spectra from laser plasmas with target of different elements," Appl. Phys. Lett. **49,** 377 (1986).
21. M. A. Duguay, "Soft x-ray lasers pumped by photoionization," Rep. SAND75-5591 (Sandia Laboratories, Albuquerque, N.M., 1975).
22. R. G. Caro, J. C. Wang, J. F. Young, and S. E. Harris, "The use of laser-produced soft x-rays for the production of excited metastable ions," Phys. Rev. A **30,** 1407 (1984).
23. R. G. Caro, P. J. K. Wisoff, D. J. Walker, M. H. Sher, C. P. J. Barty, J. F. Young, and S. E. Harris, "Soft x-ray pumping of inner-shell excited levels for extreme ultraviolet lasers," in *Short Wavelength Coherent Radiation: Generation and Applications*, D. T. Attwood and J. Bokor, eds. (American Institute of Physics, New York, to be published).
24. J. C. Wang, R. G. Caro, and S. E. Harris, "Novel short-pulse photoionization electron source: Li(1s2s2p) $^4P°$ deexcitation measurements in a plasma," Phys. Rev. Lett. **51,** 767 (1983).
25. J. K. Spong, J. D. Kmetec, J. F. Young, and S. E. Harris, "Laser spectroscopy of core-excited levels of neutral rubidium," submitted to Phys. Rev. Lett.
26. L. J. Zych, J. Lukasik, J. F. Young, and S. E. Harris, "Inelastic collisions by intense laser radiation," in *Multiphoton Processes*, J. H. Eberly and P. Lambropoulos, eds. (Wiley, New York, 1977), pp. 397–402.
27. S. E. Harris, J. F. Young, A. J. Mendelsohn, D. E. Holmgren, K. D. Pedrotti, and D. P. Dimiduk, "Quasi-metastable energy levels and applications," in *Laser Spectroscopy VII*, T. W. Hänsch and Y. R. Shen, eds. (Springer-Verlag, New York, 1985), pp. 162–165.
28. J. E. Rothenberg, J. F. Young, and S. E. Harris, "High-resolution extreme-ultraviolet spectroscopy of potassium using anti-Stokes radiation," Opt. Lett. **6,** 363 (1981).

29. J. E. Rothenberg, J. F. Young, and S. E. Harris, "Spontaneous Raman scattering as a high-resolution XUV radiation source," IEEE J. Quantum Electron. **QE-19,** 1795 (1983); erratum, **QE-20,** 986 (1984).

30. M. W. Mansfield, "The K I absorption spectrum in the vacuum ultraviolet: $2p$ subshell excitation," Proc. R. Soc. London Ser. A **346,** 539 (1973).

31. R. W. Falcone, J. R. Willison, J. F. Young, and S. E. Harris, "Measurement of the He $1s2s\ ^1S_0$ isotopic shift using a tunable VUV anti-Stokes light source," Opt. Lett. **3,** 162 (1978).

32. J. R. Willison, R. W. Falcone, J. F. Young, and S. E. Harris, "Laser spectroscopy of metastable extreme-ultraviolet levels in lithium atoms and ions," Phys. Rev. Lett. **47,** 1827 (1981).

33. C. F. Bunge, "Absolute term values for the quartet states of neutral lithium," Phys. Rev. A **23,** 2060 (1981).

34. C. F. Bunge, "Accurate calculations for the even-parity core-excited ^2P states of neutral Li," Phys. Rev. A **19,** 936 (1979).

35. R. Jáuregui and C. F. Bunge, "Emission spectrum of core-excited Li doublets," Phys. Rev. A **23,** 1618 (1981).

36. L. Engström, L. P. Somerville, and H. G. Berry, "Lifetime measurements of core-excited quartet levels in Na I," Phys. Rev. A **32,** 1468 (1985).

37. K. J. Pedrotti, "Atomic spectroscopy for soft x-ray lasers," Ph.D. dissertation (Stanford University, Stanford, California, 1985).

38. W. T. Silfvast, J. J. Macklin, and O. R. Wood II, "High-gain inner-shell photoionization laser in Cd vapor pumped by soft-x-ray radiation from a laser-produced plasma source," Opt. Lett. **8,** 551 (1983).

39. W. T. Silfvast, O. R. Wood II, H. Lundberg, and J. J. Macklin, "Stimulated emission in the ultraviolet by optical pumping from photoionization-produced inner-shell states in Cd$^+$," Opt. Lett. **10,** 122 (1985).

40. E. J. McGuire, "Soft-x-ray amplified spontaneous emission via the Auger effect," Phys. Rev. Lett. **35,** 844 (1975).

41. A. J. Mendelsohn and S. E. Harris, "Proposal for an extreme-ultraviolet selective autoionization laser in Zn III," Opt. Lett. **10,** 128 (1985).

42. D. J. Walker, R. G. Caro, and S. E. Harris, "Proposal for an extreme-ultraviolet Auger laser at 63.8 nm in Cs III," J. Opt. Soc. Am. B **3,** 1515 (1986).

43. J. F. Young, J. J. Macklin, and S. E. Harris, "Grazing incidence ellipsoidal reflector for longitudinally pumping short wavelength lasers," Opt. Lett. **12,** 90 (1987).

44. Y. Accad, C. L. Pekeris, and B. Schiff, "S and P states of the helium isoelectronic sequence up to $z = 10$," Phys. Rev. A **4,** 516 (1971).

45. L. A. Vainshtein and U. I. Safronova, "Energy levels of He- and Li-like ions (states $1snl$, $1s^3nl$ with $n = 2$–5)," Phys. Scr. **31,** 519 (1985).

46. V. Pejcev, D. Rassi, K. J. Ross, and T. W. Ottley, "High-resolution ejected electron spectrum of rubidium vapor autoionizing levels excited by electron with kinetic energies in the range 27 to 400 eV," J. Phys. B **10,** 1653 (1977).